



Faculty of Technology and Science
Department of Physics and Electrical Engineering

Helena Johansson

Nocturnal cooling

Study of heat transfer from a flat-plate solar collector

Degree Project of 30 credit points
Physics

Date/Term: 2008-02-20
Supervisor: Jan Forsberg, Jens Eriksson
Examiner: Kjell Magnusson
Serial Number: 2008:1

Abstract

This thesis investigates the possibility of using an unglazed flat-plate solar collector as a cooling radiator. The solar collector will be connected to the condenser of a heat pump and used as cooler during nighttime. Daytime the solar collector will be connected to the evaporator of the heat pump and used as heat source. The two widely differing fields of application make special demands on the solar collector. The task is given by the heat pump manufacturer Thermia and the main objective is to find out whether a solar collector should be used as a cooler or not. The performance of the solar collector under varying environmental conditions is investigated using COMSOL Multiphysics 3.3. Only the cooling properties are investigated here. The performance of the solar collector as a heat exchanger is estimated using the effectiveness-NTU method, and the solar collector is found to be a good heat exchanger at low wind speeds. The heat transfer coefficients of the convection and radiation are determined for varying temperature and wind speeds. The convective heat transfer coefficient is lowered by tubes above the absorber plate and for a high convective heat transfer rate the solar collector surface should be smooth. For a high radiative heat transfer rate the surface needs to have a high emissivity. The cooling rate is higher from a warm surface than from a cold and since no temperature change of the heat carrier is necessary the solar collector should be kept at a high temperature.

To increase the cooling rate alterations need to be made to the solar collector that makes its heating performance deteriorate. A solar collector that can be used for cooling is not an efficient solar collector.

Contents

1. Introduction	1
1.1 Background	1
1.2 Purpose	3
1.3 Nomenclature	4
2. Theory	5
2.1 Heat transfer	5
2.1.1 General	5
2.1.2 Conduction	5
2.1.3 Convection.....	6
2.1.4 Radiation	8
2.2 Fluid dynamics	11
2.2.1 Navier-Stokes equations.....	11
2.2.2 Boundary layer theory	11
2.2.3 The Boussinesq approximation	12
2.2.4 Displacement thickness	13
2.3 Solar collectors	14
2.3.1 General	14
2.3.2 Absorber plate	14
2.3.3 Heat carrier	15
2.3.4 Cover plate	15
2.4 The heat pump	17
2.5 Heat exchangers	18
2.5.1 Constructions and flow arrangements	18
2.5.3 The effectiveness-NTU method.....	19
3. Method	21
3.1 Assumptions and limitations	21
3.2 COMSOL	22
3.2.1 Overview	22
3.2.2 Heat transfer	22
3.2.3 Fluid flow	23
3.3 Models.....	24
3.3.1 Modeling	24
3.3.2 Model 1	25
3.3.3 Model 2	27
3.3.4 Additional models	28
3.4 Convection	29
3.5 Radiation	29
3.6 Heat transfer efficiency assessment	30
3.6.1 Convection.....	30
3.6.2 Radiation	31
4. Results	33
4.1 Convection and radiation	33
4.2 Heat transfer efficiency	34
4.3 Design.....	35
5. Discussion	38
5.1 Method	38
5.2 Design.....	39
5.3 Results	40

6. Conclusions	43
7. References	45
Appendix A: Navier-Stokes equation in two dimensions	A
Appendix B: Results of all simulations.....	D

1. Introduction

1.1 Background

Today there is a desire to decrease the energy consumption and to utilize the energy from the sun. Solar collectors as a heat source are an efficient and clean way of heating water and buildings. Heat pumps are a way of utilizing low quality energy that could not have come to use otherwise. The combination of solar collector and heat pump is relatively new on the market, but shows that the components can be more efficient together than separately. Heat pumps that use solar energy as low-temperature reservoir are available from some heat pump manufacturers. The solar collectors in these systems are used as evaporators, evaporating the working fluid of the heat pump. They are a complement to another heat source, often a geothermal well as in Figure 1. In the winter time, the sun can not on its own meet the demands of all heating and hot water needs and an additional heat source is necessary.

The heat carrier in the solar collector and the working fluid in the heat pump run in separate systems. This enables the use of the solar collector separately in the summer, when the solar collector can meet the demands for hot water without the heat pump. Since the heat pump does not need to be used in the summer, its running time is lowered and that extends the life of the heat pump. If a borehole is used as a heat reservoir, the excess heat from the solar collector in the summer time can be used to heat it up. A higher temperature in the borehole gives the heat pump a higher efficiency when winter comes. In the winter the working fluid in the heat pump can be extra heated by the solar collectors, and this also increases the efficiency of the heat pump. [1]

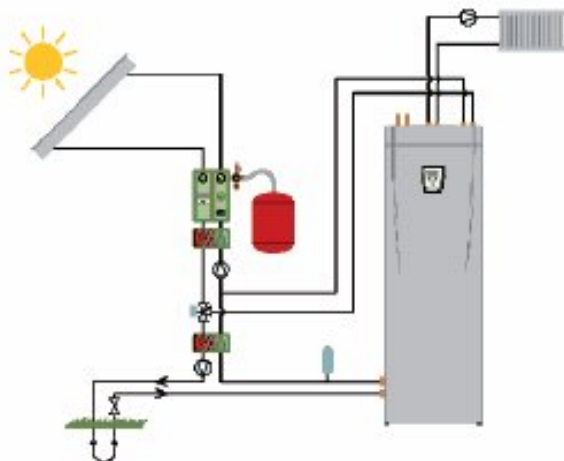


Figure 1: Image of a heat pump and solar collector system. [a]

Many heat pumps can be reversed and used to cool buildings. If a heat pump that uses a solar collector as heat reservoir should be used for cooling, the solar collector must function as condenser and cooler of the working fluid in the heat pump. This makes new demands on the design and properties of the solar collector, as the properties that make it good for heating also make it less efficient as a cooler.

The use of solar collectors as cooling radiators is an application that has been investigated before. Cooling by nocturnal radiation from roof ponds has for a long time been considered a future cheap and effective way of cooling buildings in warm climates. The roof pond absorbs heat through the ceiling and the heat is then dissipated by long wave radiation and convection. The problem with roof ponds is that they get heated during the day, but this problem can be reduced by circulating the water through cooling radiators.

Experiments described by Erell and Etzion in their article *Radiative cooling of buildings with flat-plate solar collectors*, test the properties of solar collectors used as cooling radiators. The flat-plate solar collectors are to be used only for cooling and no heating is desired. In these experiments the temperature of the heat carrier is approximately the temperature of the surrounding air. When this is the case the cooling is mainly by radiation to the atmosphere. Convection heats the solar collector if its temperature is lower than the temperature of the surrounding air. The experiment shows that available solar collectors are not ideal for cooling. In some cases vertical fins improve the convection by more than the double, in other conditions fins are less efficient and the solar collector should consist entirely of pipes. The environmental conditions, temperature difference between the solar collector and the air, and wind speed and direction are crucial to the performance. [2]

The power from the radiator is lowered if there are buildings or trees covering the sky. These objects have a higher temperature than the night sky, and since the radiative power between two objects depends on the temperature difference between the objects, see equation (12) in section 2.1.4 *Radiation*. The radiation from the radiator to the surrounding objects is lower than the radiation from the radiator to the clear sky.

1.2 Purpose

This thesis is made at the request of the heat pump manufacturer Thermia. The purpose is to investigate the heat transfer from a solar collector used as a cooler in a heat pump system. The solar collector will be used both for heating and cooling but only the cooling properties will be investigated here. The questions to be answered are;

- How does the cooling of the solar collector depend on the temperatures of the heat carrier, the surroundings and the atmosphere?
- How does varying wind speed affect the convection?
- Is convection or radiation more important for the cooling?
- Is a solar collector an efficient cooler and is there a type of solar collector that is better than others for cooling?

The main objective is to find out whether or not a solar collector should be used as a cooler.

The simulation program COMSOL Multiphysics 3.3 will be used for simulating the solar collector under varying conditions.

1.3 Nomenclature

A	Area [m ²]
B	Width of a channel or fluid volume [m]
C _c	Heat capacity rate of the cold fluid (air) [W/K]
C _h	Heat capacity rate of the hot fluid (heat carrier) [W/K]
C _{min}	Smaller heat capacity rate [W/K]
C _{max}	Larger heat capacity rate [W/K]
C _p	Specific heat capacity [J/(kgK)]
F	Force [N]
g	Gravitational constant [9.81 m/s ²]
h	Convective heat transfer coefficient [W/(m ² K)]
h _{rad}	Radiative heat transfer coefficient [W/(m ² K)]
k	Thermal conductivity [W/(mK)]
\dot{m}	Mass flow rate [kg/s]
\vec{n}	Unit vector normal [1]
Nu	Nusselt number [1]
Pr	Prandtl number [1]
Q	Heat source [W/m ³]
\dot{Q}	Heat transfer rate [W]
\dot{Q}_{\max}	Maximum heat transfer rate [W]
R	Radiated power [W]
Re	Reynolds number [1]
T _{amb}	Ambient temperature, or equivalent sky temperature [K]
T _{c,in}	Inlet temperature of the cold fluid (air) [K]
T _{c,out}	Outlet temperature of the cold fluid (air) [K]
T _{db}	Dry bulb temperature [K]
T _{dp}	Dew point temperature [°C]
T _{h,in}	Inlet temperature of the hot fluid (heat carrier) [K]
T _{h,out}	Outlet temperature of the hot fluid (heat carrier) [K]
T _{inf}	Free-stream temperature [K]
T _s	Surface temperature [K]
T _{sky}	Equivalent sky temperature [K]
U	Overall heat transfer coefficient [W/(m ² K)]
\vec{u}	Velocity vector [m/s]
u	Velocity [m/s]
u _{av}	Average velocity [m/s]
u _{inf}	Free-stream velocity [m/s]
V	Volume [m ³]
W	Weight [N]
α	Absorptivity [1]
δ_t	Thermal boundary layer thickness [m]
δ_v	Velocity boundary layer thickness [m]
δ	Characteristic length [m]
δ^*	Displacement thickness [m]
ϵ_{rad}	Emissivity [1]
ϵ_{sky}	Sky emissivity [1]
ϵ_{NTU}	Effectiveness [1]
σ	Stefan-Boltzmann coefficient, [5.67·10 ⁻⁸ W/(m ² K ⁴)]
ρ	Density [kg/m ³]
ρ_{inf}	Density of the free-stream [kg/m ³]
ρ	Reflectivity [1]
η_{fin}	Fin efficiency [1]
μ	Dynamic viscosity [Pa·s]
ν	Kinematic viscosity [m ² /s]
τ	Transmissivity [1]

2. Theory

2.1 Heat transfer

2.1.1 General

There are three ways in which heat can be transferred from one body to another. These are conduction, convection and radiation. Conduction occurs within a solid or a fluid or between bodies in contact with each other when there is no fluid flow. Convection is the heat transfer from a solid object to a fluid or within the fluid when there is fluid motion. There are two types of convection; natural convection for which the fluid motion is caused by buoyancy forces, and forced convection for which the fluid is forced to flow over the surface by for instance a fan or the wind.

Radiation, as opposed to conduction and convection, does not need a medium to take place and is the heat transfer between objects that are not in contact. [3e]

2.1.2 Conduction

Conduction is the transfer of energy as a result of interactions between particles of different energy. The rate of heat conduction through a medium depends on the geometry and material of the medium and the temperature difference across it. The equation that describes heat conduction is called Fourier's law [3e]:

$$\rho C_p \frac{\partial T}{\partial t} + \nabla \cdot (-k \nabla T) = Q \quad [4] \quad (1)$$

At steady state conditions the first term becomes zero. Q (W/m^3) is a heat source term. [4] T (K) is the temperature. Heat is conducted in the direction of decreasing temperature and hence the temperature gradient in Fourier's law is negative when temperature decreases in the positive direction of space. In order to make the conduction positive in the positive direction of space, a negative sign is added to the relation.

The thermal conductivity, k ($\text{W}/(\text{mK})$), of a material is the rate of heat transfer through a unit thickness of the material per unit area per unit temperature difference. It is a measure of how fast heat will propagate in that material. The thermal conductivity is temperature dependent. For gases it increases with increasing temperature, and for liquids it decreases with increasing temperature. The exception to this is water, whose thermal conductivity increases with increasing temperature.

The thermal diffusivity is a measure of how fast heat diffuses through a material. It is the ratio of the heat conducted through the material to the heat stored per unit volume. [3e]

2.1.3 Convection

Convection is the combined effect of conduction and fluid motion. At the surface between a solid and a fluid, the heat transfer through the fluid is by conduction, since there can be no fluid movement on the surface. This condition of a motionless fluid layer adjacent to the surface is called the no-slip condition. Because of this a boundary layer develops. [3b] A description of boundary layers follows in section 2.2 *Fluid dynamics*. At the point of contact the fluid and the solid surface must have the same temperature. This is known as the no-temperature-jump condition. [3b]

The rate of convection depends on the dynamic viscosity, thermal conductivity, density, specific heat and velocity of the fluid. It also depends on the roughness of the object surface, the geometry of the object and whether the fluid flow is laminar or turbulent. Despite the complex behavior of convection it can be described by the simple relation known as Newton's law of cooling:

$$\dot{Q} = hA(T_s - T_{\text{inf}}) \quad (2)$$

The difficulty lies in finding the correct value of h (W/(m²K)), the convective heat transfer coefficient. [3g]

The heat transfer rate depends on the flow velocity of the fluid, and for that reason an external source of flow enhancement, such as a fan or a pump, is often used to increase the rate of heating or cooling. If that is the case the heat transfer is by forced convection. The heat transfer rate at forced convection can be described with dimensionless numbers; the Reynolds number, Re, the Nusselt number, Nu and the Prandtl number, Pr. [3g]

The Reynolds number is the ratio between the inertia forces and the viscous forces in a fluid. The characteristic length δ is the tube diameter in the case of flow in a tube and the length of the plate in the flow direction in the case of flow over a flat plate.

$$\text{Re} = \frac{u_{\text{av}} \delta}{\nu} \quad (3)$$

It is used to express the turbulence intensity of the fluid. At large Reynolds numbers the flow is turbulent and at small Reynolds numbers

the flow is laminar. The transition between laminar and turbulent is not abrupt but takes place within a transition zone. [3g]

For internal flow through a tube the transition from laminar to turbulent flow begins at $Re=2300$. At $Re>4000$ the flow is fully turbulent. [3c]

When the flow is over a flat plate the transition begins is $Re\approx 5\cdot 10^5$. [3g]

The Nusselt number is defined as the ratio of the convective heat flux \dot{q}_{conv} , through the boundary layer and the conduction on the surface \dot{q}_{cond} . It is used as the dimensionless convection heat transfer coefficient.

$$Nu = \frac{\dot{q}_{conv}}{\dot{q}_{cond}} = \frac{h\delta}{k} \quad (4)$$

The heat transfer through a fluid layer is enhanced by the convection. The enhancement is described by the Nusselt number. A Nusselt number of 1 represents pure conduction, which is equivalent to a stagnant fluid layer. The larger the Nusselt number the larger the convection. δ is the characteristic length. For flow over a plate it is the length of the plate in the flow direction. [3g]

When a fluid flows over a surface a thermal boundary layer and a velocity boundary layer are formed, see section 2.2 *Fluid dynamics*. The velocity and thermal boundary layers develop simultaneously and the velocity boundary layer relative to the thermal boundary layer will have a large effect on the convection heat transfer.

The dimensionless Prandtl number is defined as the ratio of the thickness of the velocity boundary layer to the thermal boundary layer. [3g]

$$Pr = \frac{\mu C_p}{k} \quad (5)$$

Based on the Nusselt, Reynolds and Prandtl numbers, the average heat transfer coefficient, h , can be determined for a flat plate of known length L . k is the thermal conductivity of the fluid. The relations below are empirically developed for laminar and turbulent flow. [3g]

$$\text{Laminar flow: } Nu = \frac{hL}{k} = 0.664 Re^{0.5} Pr^{1/3} \quad Re < 5 \cdot 10^5 \quad (6)$$

$$\text{Turbulent flow: } Nu = \frac{hL}{k} = 0.037 Re^{0.8} Pr^{1/3} \quad \begin{matrix} 0.6 \leq Pr \leq 60 \\ 5 \cdot 10^5 \leq Re \leq 10^7 \end{matrix} \quad (7)$$

[3g]

In the absence of boundary fluid forces caused by wind or a fan, the convective heat transfer that takes place is called natural convection. When a warm object is placed in a colder fluid, heat will be transferred from the outer surfaces of the object to the adjacent layer of the fluid. As this fluid is heated, its density decreases locally and it becomes lighter than the surrounding fluid. The lighter fluid will rise, and be replaced by colder fluid from the surroundings. This flow will continue until the object is cooled to the temperature of the fluid.

If a cold object is placed in a warmer fluid, the adjacent fluid layers will be cooled down. As the colder fluid has a higher density it will sink and warm fluid flows into its place.

Natural convection is due to the buoyancy force, which is the force exerted on a body or a volume of the fluid, by a surrounding fluid. The buoyancy force, $F_{buoyancy}$, equals the weight of the fluid displaced by the body or fluid volume.

$$F_{buoyancy} = \rho_{fluid} g V_{body} \quad (8)$$

The net force, F_{net} , acting on a body completely or partially immersed in a fluid can be expressed as:

$$F_{net} = W - F_{buoyancy} = (\rho_{body} - \rho_{fluid}) g V_{body} \quad (9)$$

when there are no other forces present. W is the weight of the body. [3h]

2.1.4 Radiation

Thermal radiation is continuously emitted by all objects with a temperature above absolute zero. It is defined as electromagnetic radiation with wavelengths from 0.1 to 100 μm . This includes the infrared, the visible and part of the ultraviolet spectra. The power of electromagnetic radiation is inversely proportional to its wavelength.

When radiation is incident on a surface, three things can happen. The radiation can be absorbed, reflected or transmitted. The fraction of the incoming radiation that is absorbed by the surface is determined by the absorptivity α , the reflected fraction is determined by the reflectivity ρ , and the transmitted fraction is determined by the transmissivity τ . The sum of the absorbed, reflected and transmitted fractions of the radiation equals unity. [3i]

$$\alpha + \rho + \tau = 1 \quad (10)$$

For an opaque surface the transmissivity is zero. The properties of a surface are different in different directions and wavelengths. The

reflectivity and transmissivity depend on the angle of incidence. The absorptivity is strongly dependent on the wavelength of the incoming radiation. A way of simplifying radiation calculations is by using the grey and diffusive approximations. The diffuse approximation assumes that the properties are independent of direction, and the grey approximation assumes that the properties are independent of wavelength. In these approximations α , ρ and τ are the average properties of a medium for all directions and all wavelengths respectively. [3i]

Another radiation property is the emissivity, which gives a measure of how closely a real surface resembles that of a blackbody. It is defined as the ratio of the actual emitted power and the power that would be emitted by a blackbody at the same temperature. [5] The emissivity of a surface is different in different directions and it is temperature dependent. The gray approximation is however often used. That means that the emissivity is taken to be independent of the wavelength of the emitted radiation. [3i] A blackbody is a perfect absorber; it does not reflect or transmit any incoming radiation. It is also a perfect emitter; all of the absorbed radiation is emitted under stationary conditions. For a blackbody the absorptivity and the emissivity equal unity. [3i] The emissive power is expressed by the Stefan-Boltzmann law:

$$\dot{Q} = \varepsilon \sigma A T^4 \quad [3e] \quad (11)$$

The rate of net radiation heat transfer of a surface is the difference between the energy lost and gained by radiation. If a surface of area A , emissivity ε and temperature T_s , is completely surrounded by another surface of temperature T_{amb} , the net radiation heat transfer between these two surfaces is given by:

$$\dot{Q} = \varepsilon \sigma A (T_s^4 - T_{amb}^4) \quad [3e] \quad (12)$$

Another way of expressing the radiative power of a surface is by a relation of the same form as convection; as a product of the area, the temperature difference between the two surfaces, and a constant. It is convenient to have radiation and convection on the same form for comparisons. [5]

$$\dot{Q} = h_{rad} A (T_s - T_{amb}) \quad (13)$$

$$h_{rad} = \varepsilon \sigma (T_s^2 + T_{amb}^2) (T_s + T_{amb}) \quad (14)$$

The nocturnal radiation is the radiation between the earth surface and the night sky. The radiation comes from various gases in the atmosphere, mainly water vapor. The contributions from CO₂, ozone and other

greenhouse gases are small compared to the water vapor due to the lower concentrations.

For an accurate estimation of the atmospheric temperature, several empirical models have been developed from statistical data. One of them was developed by Berdahl and Fromberg in their article “The thermal radiance of clear skies” from Solar Energy, which is cited in [6]

$$\varepsilon_{sky} = \frac{R}{\sigma T_{db}^4} \quad (15)$$

$$T_{sky} = \varepsilon_{sky}^{1/4} T_{db} \quad (16)$$

$$\varepsilon_{sky} = 0.741 + 0.62 \left(\frac{T_{dp}}{100} \right) \quad (17)$$

In equation (15) and (16) the dry bulb temperature, T_{db} , is in Kelvin, in equation (17) the dew point temperature, T_{dp} , is in Celsius.

As the cloud cover or the humidity of the air increases, the equivalent sky emissivity ε_{sky} approaches unity. At 100 % relative humidity the equivalent sky temperature equals the dry bulb temperature. [6] The dry bulb temperature is the air temperature measured by a dry thermometer.

2.2 Fluid dynamics

2.2.1 Navier-Stokes equations

Navier-Stokes equation (18) and the continuity equation (19) are the general equations of fluid motion. They relate the velocity, pressure and outer forces in the flow of an incompressible viscous fluid. Viscosity is the internal resistance to flow, or the stickiness of the fluid. It is caused by the cohesive forces between molecules in liquids and by molecule collisions in gases. All fluids are viscous, but in some flows the viscous effects are very small and can be neglected, which greatly simplifies the analysis.

Incompressible means that the density is independent of pressure. Liquids are in general incompressible and gases can be treated as incompressible if their flow velocity is lower than 30 % of the velocity of sound in that gas. [3b]

$$\rho \left(\frac{\partial}{\partial t} + \vec{u} \cdot \nabla \right) \vec{u} = -\nabla p + \mu \nabla^2 \vec{u} + \vec{F} \quad [5] \quad (18)$$

$$\frac{\partial \rho}{\partial t} + \nabla \cdot (\rho \vec{u}) = 0 \quad [5] \quad (19)$$

The continuity equation (19) states that the mass is conserved in a fluid volume element. The Navier-Stokes equation (18) is a non-linear partial differential equation. Because of the non-linearity, solutions are very difficult to find. Most knowledge of fluid dynamics has been gathered from observations. [7] An explanation of Navier-Stokes equation is found in Appendix A.

2.2.2 Boundary layer theory

A fluid volume can be divided into a boundary layer near the surface where the friction effects are significant, and an outer layer where friction effects are negligible. [3b] This was discovered by Prandtl in 1904, and it was a great contribution to fluid mechanics because it simplifies the calculations.

At the solid surface the flow velocity of dense fluids must equal the velocity of the surface, due to the no-slip condition.

The velocity boundary layer is defined as the region in which the fluid velocity varies from zero to 99 % of the fluid velocity in the free-stream u_{inf} . [3d] Figure 2 shows the velocity profile of the boundary layer.

$$u = 0.99u_{\text{inf}} \quad (20)$$

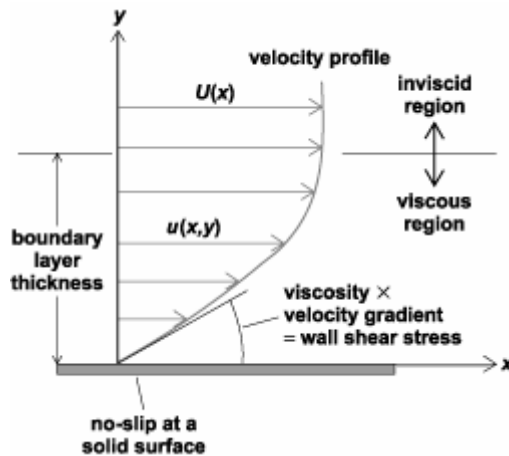


Figure 2: Velocity profile of the boundary layer. [b]

The thermal boundary layer forms as the fluid adjacent to the surface is heated by conduction, and this fluid exchanges heat with its adjacent fluid particles. A temperature profile ranging from the surface temperature to the incoming fluid temperature will arise.

The thermal boundary layer is defined as the region where the temperature difference between the fluid T and the surface T_s equals 99 % of the temperature difference between the free-stream temperature T_{inf} and the surface temperature. [3g]

$$T - T_s = 0.99(T_{inf} - T_s) \quad (21)$$

When a fluid is forced to flow at high velocity over a convex surface, the boundary layer will detach from the surface of the body. This is called separation and it is difficult to predict where it will occur, unless there are sharp corners or edges on the body. In the region behind a body, where the fluid flow has separated from the body, the velocity is reduced. This region of reduced fluid velocity is called a wake. [3d]

2.2.3 The Boussinesq approximation

When solving Navier-Stokes equation an approximation can be made by the Boussinesq approximation. This means that the density is set to a constant value in the equation, but varied in the force term. All effects of density are ignored except for the gravitational force that density variations cause. The continuity equation (19) is reduced to $\nabla \cdot \vec{u} = 0$.

$$\vec{F} = g(\rho_{inf} - \rho) \quad (22)$$

$$\rho = \rho_{inf} \left(1 - \frac{T - T_{inf}}{T_{inf}} \right) \quad (23)$$

The force \vec{F} is the gravitational force, it is in the y-direction. The density ρ depends on the density of the free-stream ρ_{inf} , on the temperature of the free-stream T_{inf} , and on the temperature T at the specific point. The expression of ρ in equation (23) is used in equation (22). The gravitational force \vec{F} is used in Navier-Stokes equation (18) as an approximation of the effects of the buoyancy force, see equation (9). [7]

2.2.4 Displacement thickness

The concept of displacement thickness is used when a viscous flow is approximated by an inviscid flow. In the velocity boundary layer the flow is governed by viscous forces. The velocity boundary layer can be replaced by a displacement thickness region in which the fluid flow is stagnant. Outside this region the velocity is the free-stream velocity, unaffected by the surface. This approximation is the same as moving the surface of the body parallel to itself a distance δ^* , and having an inviscid fluid flow right outside the surface.

The actual volume flow between the surface and a point outside the boundary layer equals the volume flow between the surface and the displacement thickness δ^* , assuming that the flow velocity in the displacement region is the same as the free-stream velocity.

The right-hand side of equation (19) gives the left-hand area in Figure 3, and the left-hand side of the same equation gives the right-hand area of Figure 3. [8a]

$$u_{inf} \delta^* = \int_0^{\infty} (u_{inf} - u(y)) dy \quad (24)$$

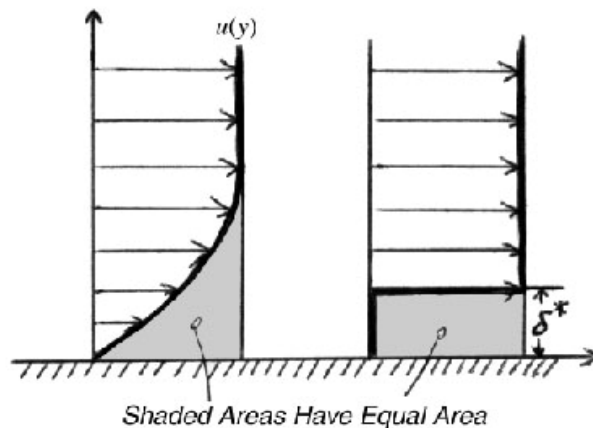


Figure 3: Velocity distribution for a real fluid and the displacement thickness. [c]

2.3 Solar collectors

2.3.1 General

Solar collectors are one of the cleanest sources of energy for space heating and hot water production. They are also efficient, as solar collectors utilize up to 50 % of the incoming solar radiation. The downside of solar energy is of course that it is out of phase with the heating needs. When the heating needs are at their peak, the supply of solar energy is at its lowest. However, the hot water needs do not vary over the year and solar collectors can be used for producing hot water during the summer.

Today there are two main solar collector designs for space heating and hot water supply; the flat-plate solar collector and the vacuum tube solar collector. The flat-plate solar collector is the traditional type and is still the most common one in use. The increasingly popular vacuum tube solar collector has a higher efficiency but is more expensive due to the higher production costs. [9] Here only the flat-plate solar collector will be described.

A typical flat-plate solar collector consists of tubes through which the heat carrier is transported, an absorber plate that absorbs incoming radiation and a cover plate that prevents outgoing thermal radiation and convective losses. The tubes can lie beneath or on top of the absorber plate, or be integrated in it. The importance is that there is good thermal contact between the tubes and the plate. The arrangement of the tubes can be as in Figure 4, or in a meandering fashion. It is important that the solar collector is well insulated on the downside and around the side surfaces, to stop heat loss.

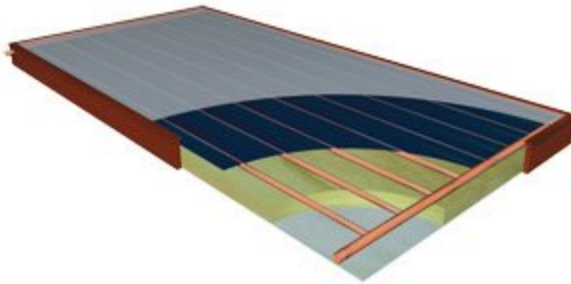


Figure 4: An image of a flat-plate collector with the tubes, absorber plate and cover plate. [d]

2.3.2 Absorber plate

The plate and tubes of a flat-plate solar collector are made of a metal with high thermal conductivity such as copper or aluminium. The high thermal conductivity is necessary for a good heat transport through the plate and to the heat carrier. [10] The ideal absorber plate has a surface with a high

absorptivity to absorb as much as possible of the incoming radiation, and a low emissivity of thermal radiation to reduce the radiative losses. A surface that has different properties in absorption and emission is called selective. Black paint has a high absorptivity but also an equally high emissivity and for that reason painting the plate black is not enough. Black paint is not selective. To achieve these demands, the surface of the plate is coated with selective coatings. [11] Solar absorbers are based on two layers with different optical properties. A typical selective surface consists of a thin upper layer which is highly absorbent to solar radiation and relatively transparent to thermal radiation, deposited on a surface that has a high reflectivity and a low emissivity for thermal radiation. Another alternative is to coat a non-selective highly absorbing material with a heat mirror having a high solar transmittance and a high infrared reflectance. [10]

Black chrome is a common selective material. It consists of microscopic chromium particles plated on a metal substrate. The chromium particles reflect thermal radiation, but solar radiation with its shorter wavelength can pass between the particles. [11]

2.3.3 Heat carrier

The heat carrier of a solar collector must not freeze in the winter, and if the flow becomes stagnant high fluid temperatures must not cause high pressure in the tubes. The most common heat carrier in solar collectors is a mix of water and glycol, with additives that prevent corrosion.

Previously ethylene glycol was most common [10], but now propylene glycol is frequently used. It has the advantage of being less toxic than ethylene glycol. [12] The flow rate through the solar collector is mostly controlled by a pump. In some solar collector models the flow is caused by the temperature difference between inlet and outlet and the rise of the hot fluid. This is called thermo-siphoning. The fluid flow rate through a 2 m² flat-plate solar collector is in the range of some liters per minute.

Operating the solar collector at a lower temperature increases its efficiency since it reduces heat losses. [10]

2.3.4 Cover plate

Glass is almost completely transparent to light, but nearly opaque to thermal radiation and prevents re-radiation from the absorber plate. For that reason it is the most common cover material for solar collectors.

It is desired that a large part of the incoming radiation is transmitted through the cover and used to heat the heat carrier. This means that the transmissivity of the cover must be high, and the reflectivity and absorptivity must be low.

The reflectivity of a material depends on its refractive index and the angle of incidence of the incoming radiation. The transmittance is at its highest

when the incoming radiation is perpendicular to the surface of the cover, increasing the angle of incidence increases the reflection.

By lowering the refractive index of the cover the reflectivity is lowered and this gives a higher transmissivity. By either coating the glass with a thin film of a material with a low refractive index, or by etching the surface to make it porous and thereby lowering the refractive index, the reflectivity of the glass is lowered.

For improved insulation multiple glasses can be used, but each glass sheet increases the reflectivity. [11]

If the cover absorbs radiation, its temperature rises and radiation and convection losses from the cover increases. [10] To absorb as little light as possible the cover material should be colorless. Window glass has a slight green tone that makes it absorb about 5-10 % of the incoming radiation. For that reason it is never used in solar collectors. The glass used for solar collectors absorbs less than 1 %. [11]

Most clear plastics are too sensitive to ultra-violet radiation to be useful as cover plates. They are also sensitive to the high temperatures that can be reached by solar collectors. [11] Another disadvantage of plastic is that its transmissivity to thermal radiation can be as high as 0.40 at some wavelengths, [10] as compared to 0.01 for glass. [11]

Recent development of transparent insulating materials will improve the efficiency of flat-plate solar collectors so that they can be comparable to vacuum tube solar collectors, but this technology is not yet commercially available. [10]

Electrochromism is the ability of a material to change its optical properties under the influence of an electric field. Experiments show a change in transmissivity from 0.74 to 0.31 at a wavelength of 775 nm, for a device made up of layers of tungsten oxide and nickel oxide. It is believed that this technology will come to great use in solar applications such as “smart windows”. [13]

2.4 The heat pump

The heat pump has gained popularity as an energy efficient way of heating buildings. It uses low-temperature, low-quality energy from the outside air, the ground or from geothermal wells. The general idea of a heat pump is to transfer heat from a colder reservoir to a warmer reservoir.

Like a heat pump, an air conditioner transfers heat from a colder to a warmer environment, but in this case the colder environment is a room or a building and the warm environment is the outdoors. Many heat pumps are designed to also function as air conditioners, cooling the home in the summer.

A working fluid is pumped around in a closed system in the heat pump. The working fluid is alternately evaporated and condensed. The heat pump operates on the vapor compression cycle, which is the most frequently used refrigeration cycle. It involves the following four ideal thermodynamic processes:

- Isentropic compression in the compressor
- Constant-pressure heat rejection in the condenser
- Throttling in an expansion device
- Constant-pressure heat absorption in an evaporator

During the compression the temperature of the heat pump working fluid increases to well above the temperature of the surrounding medium. Heat is rejected to a space heating system or to the air inside the building during the condensation. The pressure of the working fluid is reduced by an expansion device. Heat is absorbed from the outdoors, from a geothermal well or from solar collectors, to evaporate the working fluid in the evaporator. [3a]

2.5 Heat exchangers

2.5.1 Constructions and flow arrangements

The simplest type of heat exchanger consists of two concentric tubes with different diameter. It is called a double-pipe heat exchanger and it can have two different flow arrangements. In parallel flow both fluids enter the heat exchanger at the same end and move in the same direction. In counter flow the fluids enter the heat exchanger at opposite ends and move in opposite directions.

The shell-and-tube heat exchanger is very common in industrial applications. It consists of a large number of tubes inside a shell. One fluid flows inside the tubes and the other around the tubes, inside the shell. The downside of the shell-and-tube heat exchanger is its large size and weight.

A large surface area is desired for improved heat transfer and for that reason heat exchangers are provided with fins in the form of metal sheets attached to the sides of the tube.

The fins improve the efficiency of the heat exchanger and enable a larger heat transfer in a smaller volume. This is of course highly desired for heat exchangers used in vehicles, where size and weight must be limited. The fins weigh up for the low heat transfer coefficient for gases and are especially common in gas-to-gas or gas-to-liquid heat exchangers.

The compact heat exchanger is specially designed to give a large heat transfer in a small volume. The common flow arrangement in compact heat exchangers is cross flow, in which the fluids move perpendicular to each other. If the cross flow is unmixed, both fluids are forced, by the fins, to move in the perpendicular direction. If the main flow direction is perpendicular but one fluid is free to move parallel to the other fluid, the flow is called mixed. A mixed flow can have other heat transfer characteristics than an unmixed flow. [3j]

The larger the fin the higher the rate of heat transfer from the fin. But as the fin size increases, the weight and cost of the heat exchanger increases and the effectiveness of the fin decreases due to decrease in fin temperature with length. The maximum heat transfer rate from the fin is reached when the fin temperature is uniform. The fin efficiency η_{fin} is defined as the ratio between the actual heat transfer \dot{Q}_{fin} , and the heat transfer if the entire fin had the same temperature as it has at the base, $\dot{Q}_{fin, max}$. [3f]

$$\eta_{fin} = \frac{\dot{Q}_{fin}}{\dot{Q}_{fin, max}} \quad (25)$$

The overall heat transfer coefficient, U ($W/(m^2K)$), accounts for the contributions of the conduction through the walls separating the fluids, and the convection between the fluids.

The rate of heat transfer at every point of a heat exchanger depends on the temperature difference at that specific point, which varies along the heat exchanger. The logarithmic mean temperature difference, LMTD, gives an equivalent temperature difference for the two fluids along the heat exchanger, and for that reason it is the mean temperature used in heat exchanger analysis. [3j]

2.5.3 The effectiveness-NTU method

The effectiveness- NTU method is a way of determining the performance of a heat exchanger when its type and size are known. The method, which was developed by Kays and London in 1955, is based on a dimensionless parameter called the heat transfer effectiveness, ε_{NTU} .

$$\varepsilon_{NTU} = \frac{\dot{Q}}{\dot{Q}_{\max}} \quad (26)$$

In equation (26) \dot{Q} is the actual heat transfer rate and \dot{Q}_{\max} is the maximum possible heat transfer rate. The heat transfer effectiveness ε_{NTU} has a value between 0 and 1 that shows how well the heat exchanger utilizes the temperature difference between the hot and cold fluid.

To determine the actual heat transfer rate an energy balance can be used and the heat transfer rates of the hot and cold fluids can be expressed as

$$\dot{Q} = C_c (T_{c,out} - T_{c,in}) = C_h (T_{h,in} - T_{h,out}) \quad (27)$$

$$\text{where } C_c = \dot{m}C_{p,c} \quad (28)$$

$$\text{and } C_h = \dot{m}C_{p,h} \quad (29)$$

are the heat capacity rates of the cold and hot fluids.

If the cold fluid is the one with the smaller heat capacity rate, then the maximum heat transfer occurs when the cold fluid is heated to the temperature of the hot fluid. If the hot fluid is the one with the smaller heat capacity rate, the maximum heat transfer occurs when the hot fluid is cooled to the temperature of the cold fluid. The maximum temperature change over the heat exchanger is the difference between the inlet temperatures of the hot and cold fluids.

The maximum heat transfer rate can be determined from the smaller heat capacity rate, C_{\min} , and the maximum temperature difference in the heat exchanger.

$$\dot{Q}_{\max} = C_{\min} (T_{h,in} - T_{c,in}) \quad (30)$$

To determine the maximum heat transfer the mass flow rates and the inlet temperatures of the two fluids are required. From the maximum heat transfer rate \dot{Q}_{\max} and the effectiveness, ε_{NTU} , the actual heat transfer rate is determined from

$$\dot{Q} = \varepsilon_{NTU} \dot{Q}_{\max} = \varepsilon_{NTU} C_{\min} (T_{h,in} - T_{c,in}) \quad (31)$$

From equation (31), the heat transfer area A (m^2) and the overall heat transfer coefficient U (W/m^2K), relations for the effectiveness can be formulated which depend on the geometry and flow arrangement of the specific heat exchanger. These effectiveness relations involve a dimensionless group called the number of transfer units, NTU.

$$NTU = \frac{UA}{C_{\min}} \quad (32)$$

The NTU number is proportional to the surface area, and for known values of U and C_{\min} NTU is a measure of the heat transfer area. A large NTU number means that the effectiveness is good but also that the heat exchanger is large.

Another dimensionless parameter which is common in effectiveness relations is the capacity ratio

$$c = \frac{C_{\min}}{C_{\max}} \quad (33)$$

The effectiveness of heat exchangers is a function of NTU and c and the relations can be plotted. For small values of NTU the effectiveness increases rapidly with increasing NTU, but for large NTU the increase slows down. Since increasing NTU means increasing size but not much increase in effectiveness, a high NTU number is not always desired if a small heat exchanger is wanted. [3j]

3. Method

3.1 Assumptions and limitations

A solar collector will be simulated with COMSOL Multiphysics 3.3. The following assumptions are made regarding the solar collector that is used for the simulations.

- The empirical relations of heat transfer described in chapter 2. *Theory* above are only valid for ideal geometries such as flat plates and straight pipes. The geometry of an actual solar collector is not ideal. For that reason numerical methods are used for finding more accurate heat transfer values for the chosen solar collector geometry.
- An unglazed flat-plate solar collector is chosen for the simulations. This type of solar collector is assumed to have better cooling qualities than the better insulated glazed flat-plate solar collector or vacuum tube solar collector. Since the solar collector will be used both for heating and cooling, the backside is kept insulated so that the heating properties do not deteriorate too much.
- When connected to a heat pump the heating temperature of the solar collector does not need to be high and a cover is not necessary. The emissivity of the plate can be high because the low temperature in the heat collector case means that the radiation will be low regardless of the emissivity.
- There are no restrictions on the temperature of the heat carrier as long as it is lower than the temperature in the condenser. The temperature in the condenser is unknown.
- An even temperature on the solar collector surface gives better cooling, so a small temperature difference between inlet and outlet is desired.
- Since it will be used mainly for heating, the solar collector should be placed on the south side of the roof. The wind speed on the side of a building is generally low during summer nights. For that reason its properties at lower wind speeds are more interesting to investigate than its properties at higher wind speeds.

3.2 COMSOL

3.2.1 Overview

COMSOL Multiphysics is a powerful tool for simulations of physical phenomena. COMSOL Multiphysics modeling is based on solving partial differential equations, PDE:s, by the finite element method, FEM. The different equations can be found in the specifically developed modules. There are modules for simulations of for example electromagnetism, fluid dynamics, acoustics and heat transfer. The different modules can be combined for simulations of more complex systems, by using the Multiphysics mode. In addition to the available modules, new equations can be formulated. The version used is COMSOL Multiphysics 3.3.

3.2.2 Heat transfer

The heat transfer module contains equations for the simulation of heat transfer by radiation, conduction and convection, separately and in combinations. The module for combinations of all three modes of heat transfer is called General Heat Transfer.

The governing equation of heat transfer through a domain in General Heat Transfer is

$$\nabla \cdot (-k\nabla T) = Q - \rho C_p \vec{u} \cdot \nabla T \quad (34)$$

The left-hand side is the conduction and the right-hand side describes a heat source in the domain, Q , and the convection. In the case of $\vec{u} = 0$ the heat transfer is by conduction only.

The convection and conduction equation above is in non-conservative form, which assumes that the fluid is incompressible. The continuity equation of the velocity field, $\nabla \vec{u} = 0$, must be fulfilled. [4] Equation (34) can be compared with equation (1) that describes conduction and equation (27) that describes convection in a heat exchanger. Radiation is not included in equation (34) because it takes place on the surface.

On a boundary the heat transfer can be set to 0 by the condition Thermal Insulation.

$$-\vec{n} \cdot (-k\nabla T) = 0 \quad (35)$$

If the temperature on a boundary is constant, the condition Temperature is used.

$$T = T_0 \quad (36)$$

The Continuity condition means that an equal amount of energy crosses the upside of a boundary as the downside of the boundary. There is no heat source or sink on a boundary set to Continuity.

$$-\vec{n}_u \cdot (-k_u \nabla T_u + \rho_u C_{p,u} \vec{u}_u T_u) - \vec{n}_d \cdot (-k_d \nabla T_d + \rho_d C_{p,d} \vec{u}_d T_d) = 0 \quad (37)$$

If there is a source or a sink on the boundary, it is set to Heat Source/Sink; this condition is used when there is radiation or convection to or from the boundary.

$$-\vec{n}_u \cdot (-k_u \nabla T_u + \rho_u C_{p,u} \vec{u}_u T_u) - \vec{n}_d \cdot (-k_d \nabla T_d + \rho_d C_{p,d} \vec{u}_d T_d) = q_0 + h(T_{\text{inf}} - T) + \varepsilon \sigma (T_{\text{amb}}^4 - T^4) \quad (38)$$

If there is a fluid flow across the boundary and the temperature is not constant, the boundary condition Convective Flux is used, which is a combination of the following two conditions.

$$\vec{q} \cdot \vec{n} = (\rho C_p \vec{u} T) \cdot \vec{n} \quad (39)$$

$$\vec{n} \cdot (-k \nabla T) = 0 \quad (40)$$

[14]

There are two different options for radiation, either between two surfaces or between one surface and its ambient surroundings. Depending on the geometry of the model the radiation is set to either surface-to-surface or surface-to-ambient. With surface-to-surface radiation it can be investigated how two surfaces or more, respond to mutual irradiation. Surface-to-ambient radiation investigates the radiation from one surface to a distant object at constant temperature, such as the atmosphere. [4]

In a two-dimensional model, it is convenient to use the out-of-plane heat transfer function for modeling the flow of heat perpendicular to the plane of the geometry.

3.2.3 Fluid flow

Fluid flow can be modeled by two modules in COMSOL Multiphysics. These are the Isothermal Navier-Stokes equations and the Non-Isothermal Navier-Stokes equations. They are chosen depending on how the temperature changes affect the properties of the fluid, and if these changes are of interest. Here only the Isothermal Navier-Stokes equation is used. The Isothermal Navier-Stokes Equations Module is found in the Chemical Engineering Module under Momentum conservation.

The governing equations of the isothermal Navier-Stokes equation in a domain are equations (41) and (42). \vec{I} is here the unit diagonal matrix.

$$\rho \vec{u} \cdot \nabla \vec{u} = \nabla \cdot \left[-p \vec{I} + \mu (\nabla \vec{u} + (\nabla \vec{u})^T) \right] + \vec{F} \quad (41)$$

$$\nabla \vec{u} = 0 \quad (42)$$

The boundary condition of the Navier-Stokes equations on the boundary between the fluid and a solid is No-Slip.

$$\vec{u} = 0 \quad (43)$$

For a boundary with constant velocity, the boundary condition is set to Velocity.

$$\bar{u} = u_0 \quad (44)$$

When the fluid velocity is not constant, the boundary condition is set to Neutral.

$$\left[-p\vec{I} + \mu(\nabla\bar{u} + (\nabla\bar{u})^T) \right] \vec{n} = 0 \quad (45)$$

The Isothermal Navier-Stokes Equations will be used in combination with the Boussinesq approximation to simulate temperature effects on the density of the fluid. [14] See section 2.2.3 *The Boussinesq approximation*.

3.3 Models

3.3.1 Modeling

The solar collector measures 1 by 2 m and its tubes and absorber plate are made of copper. The inner diameter of the tubes is 8 mm and the outer diameter is 10 mm. The thickness of the plate is 1 mm and the distance between adjacent tubes is 10 cm. The tubes are integrated in the absorber plate. Beneath the copper tubes and plate is a layer of insulation. As heat carrier a 50 % mix of water and propylene glycol is used.

Table 1: Properties of the solid materials used in the solar collector. These properties are independent of temperature.

	Density (kg/m ³)	Thermal conductivity (W/(m·K))	Heat capacity (J/(kg·K))
Copper	8700	400	385
Insulation	100	0.04	800

When solving Navier-Stokes equations, some of the solutions found will be unstable. The instabilities can be so large that they prevent the solution from converging. One of the stabilization techniques included in COMSOL Multiphysics is Artificial diffusion. Here the Artificial Diffusion type called Streamline Diffusion is used. Streamline Diffusion makes the diffusion go in the direction of the flow, which is an approximation in line with reality. [15] The type of Streamline Diffusion used is Anisotropic Diffusion with the tuning parameter set to 0.25.

Stationary analysis was used for the two main models, see sections 3.3.2 *Model 1* and 3.3.3 *Model 2*. For the models investigating natural convection no stationary solution could be found, and time dependent

analysis was used. Because of the non-linearity of the Navier-Stokes equations, natural convection is difficult to simulate.

Only in the models demonstrating the natural convection around the solar collector, density changes of air due to temperature are included. These are modeled with the Boussinesq approximation.

In all models the weak constraints are set to non-ideal. Adding weak constraints gives more accurate flux computations. Non-ideal weak constraints give better discretization than ideal constraints when derivatives occur in the constraints. [15]

3.3.2 Model 1

Model 1 shows the solar collector in cross-section (Figure 5). This model is used for investigating the forced convective heat transfer and to find the convective heat transfer coefficients at forced convection. Natural convection is not included in these simulations.

The wind is coming in from the left side of the model where the boundary conditions are Velocity and Temperature. The other sides of the air domain are set to Neutral and Convective Flux respectively.

Three different air temperatures; 10°C, 15°C and 20°C and three different wind speeds; 1 m/s, 2 m/s and 3 m/s are tested.

The density and viscosity of air are temperature dependent properties and are changed with temperature according to Table 2. The properties are constant in each simulation and do not change as the air is heated by the solar collector. The size of the air domain is chosen so that it is larger than the boundary layers.

Table 2: Properties of air. [16]

Temperature, T (°C)	Specific heat capacity, c_p (J/kg·K)	Density, ρ (kg/m ³)	Dynamic viscosity, μ (Pa·s)	Thermal conductivity, k (W/m·K)
10	1005	1.23	$17.6 \cdot 10^{-6}$	0.025
15	1005	1.21	$17.9 \cdot 10^{-6}$	0.025
20	1005	1.19	$18.1 \cdot 10^{-6}$	0.025

On the boundary between the air and the solar collector the air velocity is set to 0 by the No-slip condition. Beneath the solar collector is a layer of insulation. The boundary condition between the solar collector and the insulation is Continuity, since no heat source or sink is present on the boundary. On the other sides of the insulation layer the boundary condition is Thermal Insulation.

The upper side of the solar collector is exposed to the air and here is where convective heat transfer and radiation takes place. The emissivity of this boundary is chosen to 0.9. The ambient temperature is set to correspond to a clear night at 80 % relative humidity and a cloudy night with 100 % relative humidity.

Having two boundaries with very different temperature in contact is against the no-temperature-jump condition. In the left side of Model 1 (Figure 5), where the solar collector and the air meet, the temperature of the air is set to a specific temperature, which means that the edge of the solar collector must have the same temperature as the air. This gives a very abrupt cooling of the solar collector near this edge, and in addition forces a large amount of heat out through the boundary on the side of the solar collector, something that is not in agreement with reality. For this reason a small piece of insulation is placed at this boundary. This gives a model that is more realistic as it does not have an abrupt temperature change, and that prevents the heat transfer through the boundary.

Because of the difficulty in solving Navier-Stokes equation only part of the solar collector could be modeled. Model 1 shows 50 cm of the solar collector.

This model is simplified by replacing the heat carrier inside the tubes with a constant temperature on the boundary. It reduces the number of equations that must be solved since there is no equation to solve inside the tubes. This simplification can be made because the temperature on the boundary will be nearly constant and because the fluid flow is in the direction perpendicular to the geometry. The tested fluid temperatures are 25°C, 50°C and 75°C.

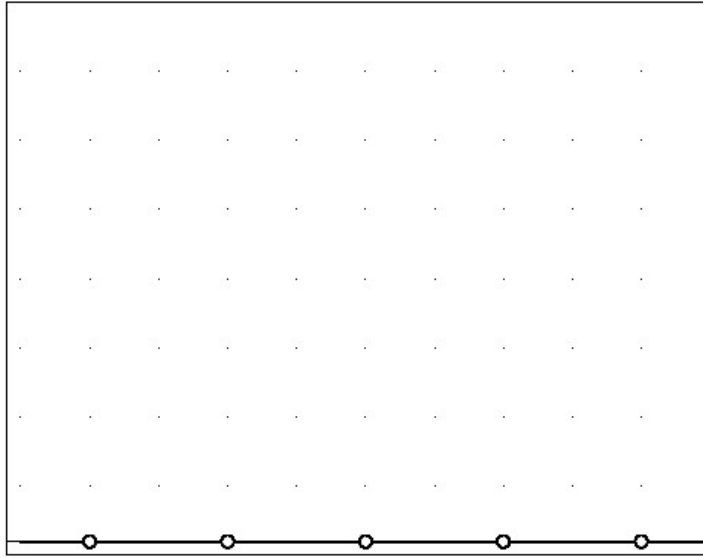


Figure 5: The first model, at the bottom at the picture is the solar collector, above that is air domain. The thin (1 cm) piece of insulation that was added to prevent temperature jumps can be seen in the left corner of the solar collector.

3.3.3 Model 2

The second model (Figure 6) shows the solar collector seen from above and is made for investigating the total heat transfer, including forced convection and radiation. The convection coefficients from the first model are used in this one. Since the natural convection is not included in the convective heat transfer coefficients, the effects of natural convection are not demonstrated in the simulations. With this model the fluid flow and the cooling of the fluid can be investigated.

The model of the solar collector seen from above is simpler to solve since it does not include an air domain. The whole solar collector (1 by 2 m) can be modeled. Instead of an air domain the convective heat transfer coefficient found in the model of the cross-section is used.

The plate between the tubes is 1 mm thick and the tubes are set to 8 mm. This is because only one layer is modeled and that is the heat carrier, the tubes are not in the model. The tubes are circular in the cross-section model, but in this model they are square, 8 mm by 8 mm. At the top and bottom of the solar collector, at the inlet and outlet, are two tubes that are 8 mm by 20 mm.

The outer boundaries of the solar collector are thermally insulated. No heat should be transferred from the back of the solar collector and the heat transfer coefficient as well as the emissivity is always zero. The emissivity of the upper side is 0.9. The out-of-plane heat transfer function is used.

The temperatures of the heat carrier and the air are varied in the same manner as for Model 1, with the heat transfer coefficient changing according to the results from the cross-section model.

The velocity of the heat carrier at the inlet is 0.21 m/s which corresponds to 2 l/min. The density, viscosity, heat conduction and heat capacity of the heat carrier are changed with temperature according to Table 3. The properties are constant in each simulation and do not change as the heat carrier is cooled down.

Table 3: Properties of a 50 % by weight mixture of water and propylene glycol. [17]

Temperature, T (°C)	Specific heat capacity, c_p (J/kg·K)	Density, ρ (kg/m ³)	Dynamic viscosity, μ (Pa·s)	Thermal conductivity, λ (W/m·K)
25	3551	1040	$5.39 \cdot 10^{-3}$	0.365
50	3648	1024	$2.29 \cdot 10^{-3}$	0.375
75	3744	1005	$1.24 \cdot 10^{-3}$	0.381

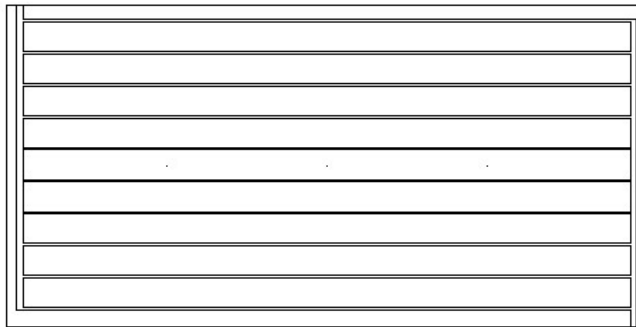


Figure 6: Model 2, the solar collector as seen from above.

3.3.4 Additional models

There is one model which demonstrates the impact of the tubes on the convective heat transfer. It shows a flat plate with a constant temperature, and is similar to the solar collector in cross-section, only that the tubes have been removed and the plate has a constant temperature. This model is used for finding the convective heat transfer coefficient at forced convection over a flat plate.

One model shows the solar collector placed on a roof with a 25° inclination, this model is for demonstrating the natural convection from the hot surface, and how it is affected by the inclination of the roof. It is simplified and shows only the air above the roof. In this model the temperature dependency of the air density is modeled with the Boussinesq

approximation. The density is varied in the equation, not only in the force term.

Another model shows the fluid motions induced by the edge of the solar collector lying on the roof. This model investigates the reduction in wind speed in the wake of the edge. In this model the density is not temperature dependent.

3.4 Convection

The convective heat transfer coefficient was found through the convective heat transfer in the model showing the cross-section of the solar collector. The normal total heat flux was integrated over the air boundaries. That value was then divided by the difference between the average temperature of the surface and the temperature of the air and by the area of the solar collector in this model.

$$h = \frac{\dot{Q}_{conv}}{A(T_{s,av} - T_{air})} \quad (46)$$

The Nusselt numbers were calculated from the convective heat transfer coefficients, the length of the plate in the specific model and the thermal conductivity of air.

$$Nu = \frac{hL}{k} \quad (47)$$

3.5 Radiation

The equivalent sky temperature was calculated from equations (15), (16) and (17). The dew point temperature was read from a Mollier diagram at 80 % relative humidity [15]. Table 4 shows the equivalent sky temperatures at the air temperatures used in the simulations. At 100 % relative humidity the equivalent sky temperature equals the air temperature.

Table 4: Equivalent sky temperature at 80 % relative humidity.

Air temperature (°C)	Dew point (°C)	ε_{sky}	Equivalent sky temperature (°C)
10	7	0.7844	-7
15	12	0.8154	1
20	17	0.8402	7

The radiative heat transfer was found from Model 2 by integrating the out-of-plane radiative heat transfer over the entire surface. That value was divided by the temperature difference between the surface and the ambient temperature and by the area of the solar collector in the specific model to give the radiative heat transfer coefficient h_{rad} .

$$h_{rad} = \frac{\dot{Q}_{rad}}{A(T_{s,av} - T_{amb})} \quad (48)$$

A comparison between the convective heat transfer coefficient, h , and the radiative heat transfer coefficient, h_{rad} , is made by taking the ratio of the radiative heat transfer coefficient to the total heat transfer coefficient.

$$Ratio = \frac{h_{rad}}{h_{rad} + h} \quad (49)$$

3.6 Heat transfer efficiency assessment

To give a measure of the quality of the heat exchanger performance of the solar collector the effectiveness-NTU method is used. The NTU method is developed for convective heat transfer and internal flow. In this case the air flow is external and there is an additional radiative heat transfer of the same size as the convective. This means that some changes have to be made to adjust the NTU method to external flow and radiation.

3.6.1 Convection

To get a proper value on the air mass flow rate it is assumed that the thermal boundary layer, which is where heat transfer takes place, can be seen as an imaginary air channel that replaces the tube or other enclosure that the NTU method is developed for. The mass flow is then the mass flow out of this imaginary enclosure, since that is the air that has taken part in the heat transfer. These assumptions are based on the theory of displacement thickness.

The mass flow rate of the air was found by integrating the outward velocity of the upper air boundary of the COMSOL model and multiplying the result by the density. However this represents the mass flow through the velocity boundary layer. The mass flow through the thermal boundary layer is found by dividing the mass flow through the velocity boundary layer by the Prandtl number.

$$\dot{m}_v = \rho \dot{V} = \rho u A = \rho \delta_v B u \quad (50)$$

$$\delta_t = \frac{\delta_v}{Pr} \quad (51)$$

$$\dot{m}_t = \frac{\rho \delta_v B u}{Pr} \quad (52)$$

$$\dot{m}_t = \frac{\dot{m}_v}{Pr} \quad (53)$$

where \dot{m}_v (kg/s) is the mass flow through the velocity boundary layer, \dot{m}_t (kg/s) is the mass flow through the thermal boundary layer, ρ (kg/m³) is the density of the air, u (m/s) is the imaginary mean velocity of the air through the imaginary channel, B (m) is the width of the channel, δ_v (m) is the height of the velocity boundary layer, δ_t (m) is the height of the thermal boundary layer and Pr is the Prandtl number, which for air at 10°C is 0.72.

The mass flow rate of the heat carrier was known, since the volume flow through the solar collector is 2 l/min, and it was found that the capacity rate of the heat carrier was larger than the capacity rate of the air. The maximum heat transfer could then be determined from the capacity rate of the air and the temperature difference between the inlet temperatures of the air and the heat carrier. From the COMSOL calculated actual heat transfer and the maximum heat transfer the effectiveness was determined.

$$\varepsilon_{NTU} = \frac{\dot{Q}}{\dot{m}_t C_{p,air} (T_{h,in} - T_{c,in})} \quad (54)$$

3.6.2 Radiation

In the case of radiative cooling there is no mass flow and no heat capacity involved, however an equivalent equation on the same form as the forced convection can be formulated. See equation (13). $h_{rad}A$ represents the capacity rate of the heat carrier.

$$\dot{Q} = h_{rad} A (T_s - T_{amb}) \quad (55)$$

Here the surface temperature T_s represents the outlet temperature of a cold fluid and the sky temperature T_{amb} represents the inlet temperature. After comparison with the capacity rate of the heat carrier, $h_{rad}A$ was found to correspond to C_{min} .

The maximum temperature difference is the difference between the inlet temperature of the heat carrier and the ambient temperature and this temperature difference will be used for finding \dot{Q}_{max} .

Since the surface temperature affects the radiative heat transfer coefficient, an $h_{rad, max}$ was calculated from the maximum surface temperature, with $\varepsilon_{rad}=1$. The temperature on the surface of the plate

corresponds to the outlet temperature of the cold fluid, so the highest heat transfer must occur when the surface of the plate is heated to the inlet temperature of the hot fluid. See equation (14) for definition of h_{rad} .

$$h_{rad, \max} = \varepsilon_{rad} \sigma (T_{in}^2 + T_{amb}^2) (T_{in} + T_{amb}) \quad (56)$$

The maximum heat transfer was calculated as

$$\dot{Q}_{\max} = C_{\min} (T_{h,in} - T_{c,in}) = h_{rad, \max} A (T_{h,in} - T_{amb}) \quad (57)$$

The actual heat transfer was determined by COMSOL. The effectiveness was determined by;

$$\varepsilon_{NTU} = \frac{\dot{Q}}{h_{rad, \max} A (T_{h,in} - T_{amb})} \quad (58)$$

4. Results

4.1 Convection and radiation

Table 5 shows the convective heat transfer coefficients calculated with the help of Model 1. As the temperature effects were small, the values in Table 5 are averages over all different temperatures. The full results of the simulations can be found in Appendix B, Table 10.

Table 5: Average values of the convective heat transfer coefficient.

Air velocity (m/s)	1	2	3
Heat transfer coefficient, h (W/m ² K)	4.64	6.17	7.24

The Nusselt numbers in Table 6 are calculated from the convective heat transfer coefficients in Table 5.

Table 6: Nusselt numbers for varying wind speed.

Air velocity (m/s)	1	2	3
Nusselt number	93	123	145

Table 7 shows the radiative heat transfer coefficient at 80 % relative humidity and at 100 % relative humidity. Changes in the relative humidity of the air only affect the radiation, not the convection. The values in Table 7 are averages over the wind speeds; 1 m/s, 2 m/s and 3 m/s. The full results of the simulations can be found in Table 11 and Table 12, Appendix B.

Table 7: The radiative heat transfer coefficients at different relative humidity

Air temperature (°C)	Fluid temperature (°C)	$h_{\text{rad, 80 \% RH}}$	$h_{\text{rad, 100 \% RH}}$
10	25	4.54	4.98
	50	5.13	5.59
	75	5.77	6.25
15	25	4.75	5.12
	50	5.36	5.74
	75	6.00	6.41
20	25	4.91	5.26
	50	5.52	5.89
	75	6.18	6.70

In Figure 7 the ratio of the radiative heat transfer to the total heat transfer is shown as averages for varying heat carrier temperature and wind speed.

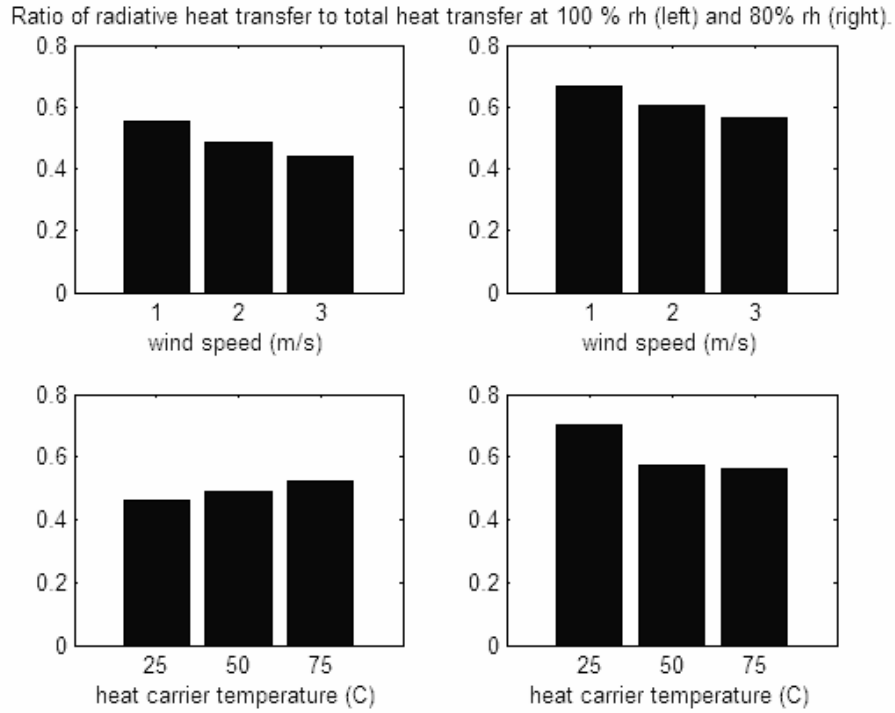


Figure 7: Ratio of the radiative heat transfer to the total heat transfer at 100 % and 80 % relative humidity.

4.2 Heat transfer efficiency

The effectiveness according to the NTU method was calculated from the heat transfer attained from COMSOL Multiphysics and the maximum heat transfer calculated with the NTU method. See Appendix B, Table 13 and Table 14 for full simulation results.

Table 8: Heat transfer efficiency for the convection, fluid temperature 50°C.

Air velocity (m/s)	1	2	3
Effectiveness, ϵ_{NTU}	1.00	0.56	0.46

Table 9: Radiation, fluid temperature 50°C, wind speed 3 m/s.

Air temperature (°C)	Relative humidity (%)	Effectiveness, ϵ_{NTU}
10	80	0.79
	100	0.77
15	80	0.79
	100	0.77
20	80	0.79
	100	0.78

4.3 Design

The simulations of Model 1 show that the tubes create wakes that lower the heat transfer rate, see Figure 8. Simulations made of a solar collector with a planar surface gives the convective heat transfer coefficient $h=8$ W/(m²K) at 2 m/s, see Appendix B, Table 13 for simulation results. A wake is also formed at the edge of the solar collector, as can be seen in Figure 9. Figure 10 shows the cooling of the absorber plate. In Figure 11 the effects of natural convection is showed for a solar collector lying on a roof with an inclination of 20°.

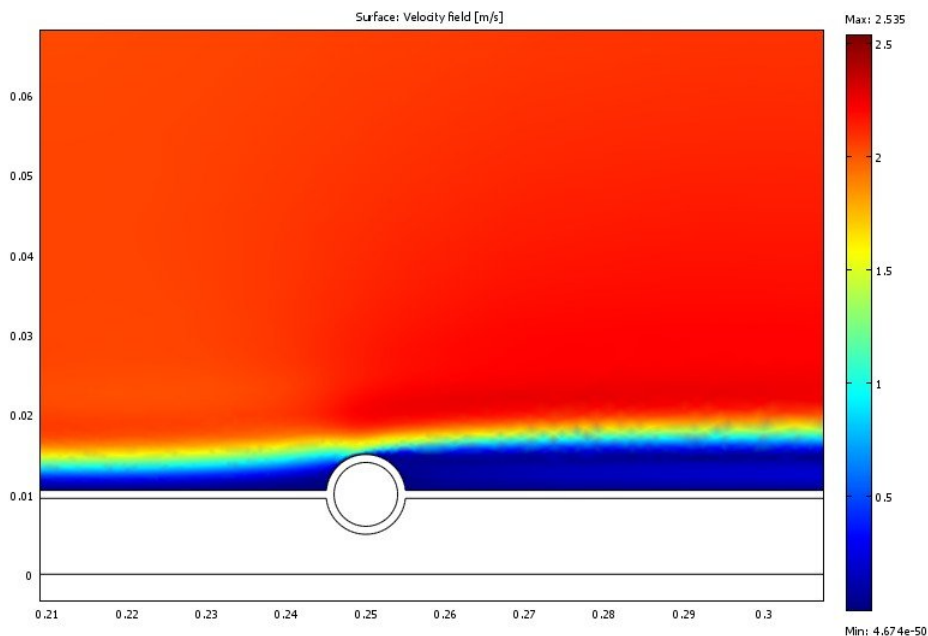


Figure 8: Image of the wake caused by the tubes.

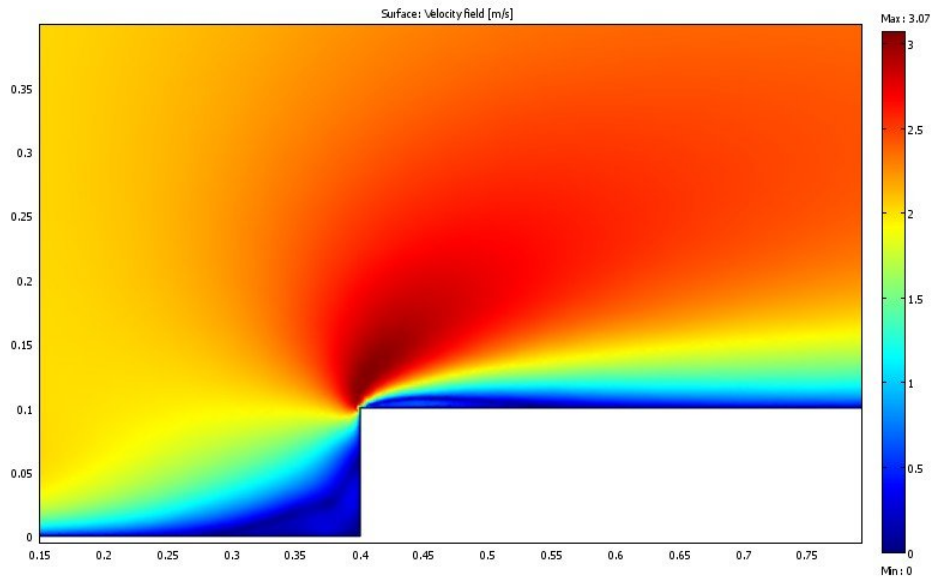


Figure 9: Image of the velocity field around the edge of the solar collector. The incoming wind speed is 2 m/s. The edge creates a wake.

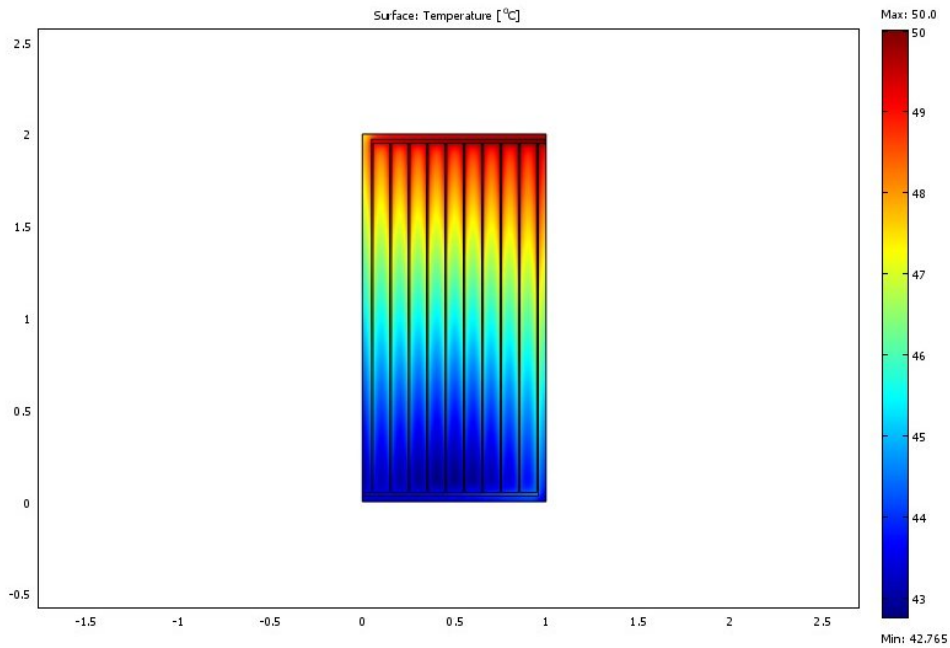


Figure 10: Image of surface temperature of the solar collector. The air temperature is 15°C, the ambient temperature 15°C, the inlet fluid temperature 50°C, the air velocity 2 m/s and the fluid flow rate 2 l/min. The temperature of the plate is lower between the tubes than by the tubes.

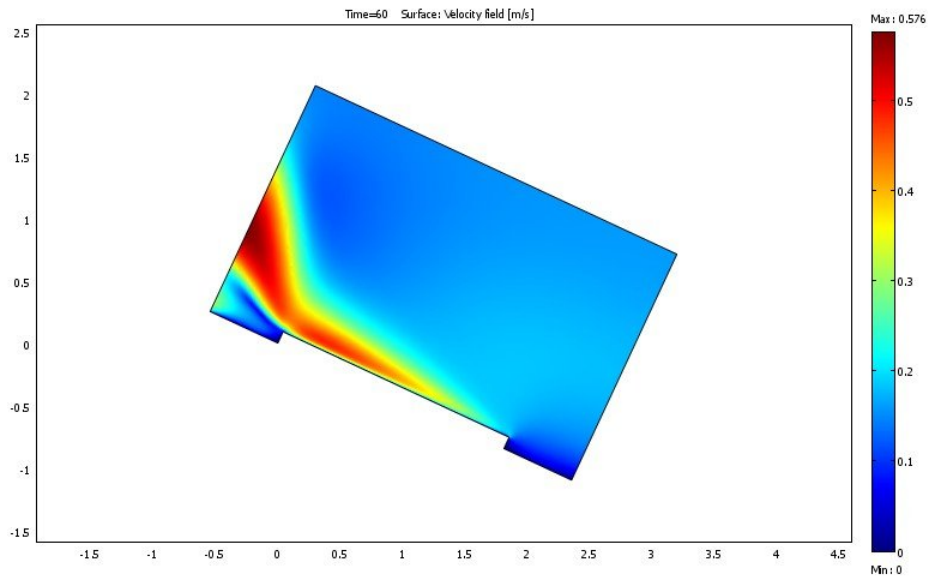


Figure 11: Image of the air flow around the solar collector on the roof, due to natural convection, after 60 s simulation. See colored bar to the right for wind speed. The temperature of the plate is 50°C and the air temperature is 10°C.

5. Discussion

5.1 Method

The difficulty when modeling fluid flow is convergence. The larger the model is the more difficult is it to make it converge. For this reason a smaller model was used for finding the convective heat transfer coefficients.

In a real application there will probably be many solar collectors lying side by side on the roof. The boundary layer will be thicker at the end of the roof, and a thicker boundary layer means a lower convective heat transfer coefficient. The convective heat transfer coefficient h obtained with this model is probably not valid for a larger solar collector. The larger size will create a thicker boundary layer and that will lower the heat transfer coefficient.

At low wind speed the natural convection is probably a significant part of the heat transfer. It can be seen from simulations (Figure 11) that natural convection causes wind speeds of 0.3 to 0.5 m/s over the solar collector surface when its temperature is 50°C. For better accuracy the temperature dependence of the air density should have been included in all of the simulations, especially the simulations with 1 m/s wind speed. However this was not possible as the models did not converge when the temperature dependence of the air density was included.

The air domain in Model 1 could have been made smaller. It only has to be larger than the boundary layer. With a smaller air domain it is easier to reach convergence. If the air domain had been made smaller perhaps the natural convection could have been included in the simulations, or the simulations could have been made with a larger model, that would have given a better value of h .

The models do not include fluid motion on the edge, which further lowers the heat transfer rate. It can be seen in Figure 10 that a wake is formed by the edge.

The NTU method was adjusted to both external flow and radiation. A mass flow had to be evaluated for the external flow, and that mass flow was chosen as the mass flow out of the thermal boundary layer. For a more reliable value on the maximum heat transfer a better estimation of the mass flow involved in the heat transfer is necessary.

The NTU method has not been used on radiation before. There is no mass flow involved in radiation and $h_{rad}A$ was used instead of a heat capacity rate. It has the same dimensions and like a heat capacity rate it is a measure of the heat transfer rate.

The effects of radiation from surrounding trees and buildings have not been considered and it is assumed to have a negative impact on the radiative heat transfer from the solar collector as they stand in the way of

the sky. Another thing that has not been considered is the fact that nights are not always completely dark. The summer nights when cooling is most desired, there is diffuse incoming radiation from the sky which will further decrease the radiative heat transfer from the solar collector.

The Boussinesq approximation was used for simulating the effects of natural convection. In the Boussinesq approximation density variations are present only as variations in the gravitational force, not in any other parts of the Navier-Stokes equation. Here the density is varied in the entire Navier-Stokes equation. Using the Boussinesq approximation as it should be used would have simplified calculations and perhaps given steady state solutions to natural convection problems.

5.2 Design

The desired properties of the solar collector differ between cooling and heating. The two greatest differences concern the glazing and the emissivity of the absorber plate. Solar collectors mostly have a glass cover as that greatly prevents heat losses, especially at high temperatures. When used for cooling, the glass cover must be removed or else there will be no convective cooling and the thermal radiation will not be transmitted through the cover.

When the solar collector is used as the heat source for a heat pump, its temperature can be lower than when its purpose is to produce hot water. If the temperature of the heat carrier is approximately the temperature of the surrounding air, a very small amount of heat will be lost to the surroundings.

An unglazed flat-plate solar collector can be used for producing hot water but its efficiency is lower than the efficiency of a glazed solar collector since the heat losses are greater.

The absorber plate of solar collectors is usually coated with a material to make it selective. It has a high absorptivity to solar radiation and a low emissivity of thermal radiation. This is a problem for a solar collector used for cooling as the thermal radiation from the surface becomes very low. Ideally, a solar collector used only for cooling should have a low absorptivity for solar radiation and a high emissivity at thermal wavelengths.

If the temperature of the solar collector is held low when it is being used for heating, the thermal radiation from it will be low regardless of the emissivity of the absorber plate.

A future alternative for solar collectors with both heating and cooling purposes is the use of electrochromic materials, whose optical properties change under the influence of an electric field. When this technology is further improved and becomes available for applications, it can perhaps

be used to improve solar collector performance and alter the properties of the cover depending on the field of application for the solar collector.

Removing the insulation from the back of the solar collector will increase the convection, but it will also cause the solar collector to heat the roof. Depending on the roof material this heat will affect the cooling as the roof reradiates heat to the solar collector. Experiments on the magnitude of this heat exchange should be made to investigate the effects of insulation compared to when there is a region of air below the solar collector. If the temperature difference between the roof and the solar collector is small, the heat exchange will be small.

For maximum heat exchanger efficiency the absorber plate, or the fins of the tubes, should have the same temperature at the centre between two tubes as it has by the edge of the tube. The fins are most efficient when their temperature is high, see equation (25). The temperature difference over the plate depends on the temperature and the flow velocity of the heat carrier. This should be considered when choosing a solar collector for cooling. Perhaps the distance between the tubes should be shorter than the 10 cm it is in this solar collector.

The solar collector in this experiment has tubes that partially protrude over the absorber plate. When the wind comes from the side of the solar collector wakes are created behind the tubes. This can be seen in Figure 8. In the wakes the wind speed is lowered and this lowers the heat transfer rate in the wakes. The heat transfer rate of a flat plate is investigated and is found to be higher than the heat transfer rate from this solar collector. A solar collector with its tubes attached beneath the absorber plate has a smooth surface and is a better alternative for cooling. Other flow arrangements than cross-flow have not been investigated, but when the air flow is parallel to the tubes there can be no wakes behind them. A smooth surface is regarded as better since it does not cause wakes.

Unglazed flat-plate solar collectors have an advantage in that they are cheaper than other solar collectors. In combination with heat pumps perhaps unglazed solar collectors can compete in efficiency with other solar collectors, since the temperature can be kept below the temperature of the surroundings. The use of unglazed solar collectors might enable cooling but they also limit the possibility of using only the solar collector, without the heat pump, for producing hot water.

5.3 Results

The convective heat transfer coefficients h found in Table 5 were determined from a model of the first 50 cm of the solar collector. The boundary layer becomes thicker with length, and a thicker boundary layer

means a lower heat transfer rate. The actual convective heat transfer coefficient is probably lower than the heat transfer coefficient found in the simulations. The convective heat transfer coefficient varies with wind speed. The dependence on solar collector temperature and air temperature is small.

The Nusselt number in Table 6 was determined from the convective heat transfer coefficient and the length of the plate in Model 1 (50 cm). The Nusselt number can be a more useful measure of the convection than the convective heat transfer coefficient since it is dimensionless.

The radiative heat transfer coefficient h_{rad} varies with the temperatures of the solar collector and the air. In this thesis the emissivity of the absorber plate was 0.9. For an actual solar collector the emissivity is lower than this because of the selective surface. The high value was chosen to improve the cooling of the solar collector but it makes the comparison with convection difficult to make. The emissivity of the solar collector surface must be considered when comparisons are made. As can be seen in Table 7, the heat transfer coefficient h_{rad} is higher when the relative humidity of the atmosphere is 100 % than it is when the relative humidity is 80 %. The reason for this is that h_{rad} increases with both surface temperature and atmospheric temperature. See equation (14) for definition of h_{rad} . At high relative humidity the atmospheric temperature takes a higher value and for that reason the value of the radiative heat transfer coefficient increases as well.

The ratio of the radiative heat transfer coefficient to the total heat transfer coefficient behaves differently at 80 % and 100 % relative humidity. At low heat carrier temperatures and low relative humidity, the ratio of the radiative heat transfer to the total heat transfer is larger than it is at high relative humidity. This can be seen in Figure 7. The reason for this is that at low relative humidity the temperature of the atmosphere is lower than the temperature of the air. Radiation then becomes more important for the cooling than convection.

The results of the heat transfer efficiency assessment show that the solar collector is a good heat exchanger, especially at low wind speed. The values of the efficiency found in Table 8, are not reliable as they depend on the maximum heat transfer which was difficult to estimate. However the analysis made with the NTU method shows that the efficiency of the solar collector as a heat exchanger decreases with increasing wind speed, and thus increasing mass flow, and this result can be considered as valid. The solar collector is a better heat exchanger at low wind speed than at high wind speed.

For the radiation the results in Table 9 show that the solar collector is a good radiator. One way of improving the radiative cooling is by increasing the emissivity of the absorber plate, another way is to maintain

the solar collector surface at a higher temperature and this can be done by increasing the flow rate of the heat carrier.

A scenario that has not been investigated is when the temperature of the heat carrier is lower than the temperature of the surroundings. In this case there will be no convective cooling of the solar collector; instead the convection will heat the heat carrier. To increase the cooling rate from the solar collectors, they need to be operated at a higher temperature than the surroundings. Heat pumps can raise the temperature of the heat carrier to above air temperature, but if the hot side reaches sufficiently high temperatures there is a possibility that the heat can come to use for example for heating water, instead of being cooled by the atmosphere. Storing the heat in a hot water tank makes better use of the energy used by the heat pump.

6. Conclusions

The higher the temperature difference between the solar collector and the surrounding air or the atmosphere, the higher the cooling rate. A high solar collector temperature gives a high cooling rate. The temperature of the solar collector depends on the temperature of the heat pump, and getting a high temperature out of the heat pump consumes power. The temperature of the solar collector should not be so high that the power consumption of the heat pump makes the system inefficient.

Whether convection or radiation is most important for the cooling rate depends on the emissivity of the solar collector, the atmospheric temperature and the wind speed. If the solar collector has a high emissivity and the atmospheric temperature and the wind speed are low, the radiation is more important. As the wind speed increases so does the convective cooling rate. At high relative humidity, convection becomes more important for the cooling rate than radiation.

The convective cooling rate is higher from a solar collector with a smooth surface than from a solar collector with tubes above the absorber plate because the tubes lower the flow velocity near the surface.

A solar collector is a good heat exchanger at low wind speed but its effectiveness decreases as the wind speed increases.

At cooling, when the absorber plate functions as cooling fins, the maximum fin efficiency occurs when the temperature of the absorber plate is the same at the centre between two tubes as it is by the tubes. This is reached by having a short distance between the tubes.

The alterations that need to be made to the solar collector to enable its use for cooling make it less efficient as a solar collector. An alternative solution to a solar collector that can be used as a cooler is separate solar collectors and cooling radiators. The cooling radiators can be specialized for cooling and be made more effective for that than solar collectors, while the solar collectors can keep their good heating properties. The cooling radiator should have a design with a smooth surface to increase convective heat transfer. The surface should have a high emissivity since that increases the radiative heat transfer.

If a solar collector can be used as a cooler in the future depends on many things. One question that needs to be answered is whether the solar collector can be operated at a lower temperature when used for heating, and if the lower temperature makes the cover glass unnecessary. The heating properties of unglazed solar collectors also need to be investigated.

In existing solar collector and heat pump systems, the solar collectors are a complement to a geothermal well (section *1.1 Background*). The well

has a low temperature and can be used for cooling. The cooling rate from the well needs to be compared to the cooling rate from the solar collector or cooling radiator to see which is more efficient.

7. References

[1] www.eviheat.se 2008-01-15

[2] *Radiative cooling of buildings with flat-plate solar collectors*, Erell, Etzion, Building and environment 35 (2000) 297-305

[3] *Fundamentals of Thermal-Fluid Sciences*, International Edition, Çengel, Turner, McGraw-Hill Companies Inc. 2001, ISBN 0-07-118152-0

- [3a] Chapter 8
- [3b] Chapter 9
- [3c] Chapter 12
- [3d] Chapter 13
- [3e] Chapter 14
- [3f] Chapter 15
- [3g] Chapter 17
- [3h] Chapter 18
- [3i] Chapter 19
- [3j] Chapter 20

[4] COMSOL, Heat Transfer Module, User's Guide

[5] *Energiteknik*, Henrik Alvarez, Studentlitteratur 1990, ISBN 91-44-31471-X

[6] *Simplified modelling of the nocturnal clear sky atmospheric radiation for environmental applications*, M. Pérez-García, Ecological modelling 180 (2004) 395-406

[7] *Physical Fluid Dynamics*, Second edition, D.J. Tritton, Oxford Science Publications, 2003, ISBN 0-19-854493-6

[8] *Introduction to fluid mechanics*, Y. Nakayama, R.F. Boucher, Butterworth-Heinemann 1999, ISBN 0-340-67649-3, pp. 103-104

- [8a] p. 103-104
- [8b] p. 82-87

[9] www.aquasol.se 2008-01-15

[10] *Solar thermal collectors and applications*, Soteris A. Kalogirou, Progress in Energy and Combustion Science 30 (2004) 231–295

[11] *Solar Thermal Engineering – Space Heating and Hot Water Systems*, Peter J. Lunde, John Wiley & Sons, Inc. 1980, ISBN 0-471-08233-3

[12] www.lesol.se 2008-01-15

[13] *Transparent conductors as solar energy materials: A panoramic review*, C. G. Grankvist, Solar energy materials and solar cells 91 (2007) 1529-1598

[14] COMSOL Multiphysics 3.3 Manual

[15] Femlab 3, User's Guide

[16] *Energitekniska formler och tabeller*, J. Berghel, R. Renström,

[17] *2005 ASHRAE Handbook – Fundamentals (SI)*, Physical properties of secondary coolants (brines)

Images:

[a]

http://www.ctcvarme.se/enertech/p45563/files/CTC_EcoSol_070921.pdf
2008-01-15

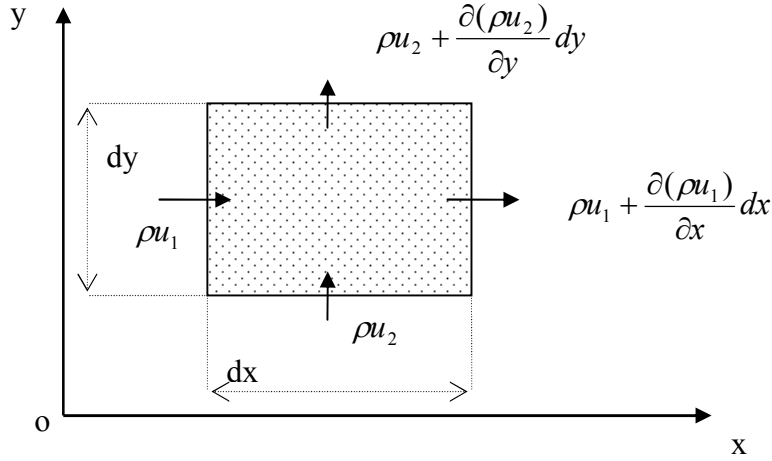
[b] <http://www.answers.com/topic/boundary-layer?cat=health> 2008-01-15

[c] <http://www.aerofkey.com/papers/bl/node2.html> 2008-01-15

[d] <http://www.regulus.eu/Ploche-slunecni-kolektory.asp> 2008-01-15

Appendix A: Navier-Stokes equation in two dimensions

In the derivation of the Navier-Stokes equations, first consider a fluid element with side lengths dx and dy and thickness b . The volume of the element is $b dx dy$. The velocities in the x and y directions are u_1 and u_2 respectively. In the fluid element there can be a mass flow in and out of the element and a mass storage inside the element. [8b]



By taking the difference between the inflow and the outflow in the x and y directions, the fluid mass stored in the respective directions per unit time can be obtained as $-\frac{\partial(\rho u_1)}{\partial x} b dx dy$ and $-\frac{\partial(\rho u_2)}{\partial y} b dx dy$ respectively. The initial mass of the fluid element is $\rho b dx dy$, and this should increase by $\frac{\partial(\rho b dx dy)}{\partial t}$. [8b]

The change in mass of the fluid element due to mass flow and mass storage is expressed in the continuity equation:

$$-\frac{\partial(\rho u_1)}{\partial x} b dx dy - \frac{\partial(\rho u_2)}{\partial y} b dx dy = \frac{\partial(\rho b dx dy)}{\partial t} \quad (\text{A.1})$$

divided by the volume of the element [8b]:

$$\frac{\partial \rho}{\partial t} + \frac{\partial(\rho u_1)}{\partial x} + \frac{\partial(\rho u_2)}{\partial y} = 0 \quad (\text{A.2})$$

Now apply Newton's second law of motion on the fluid element. The inertial force is the product of the mass and acceleration of the fluid element. The forces acting on the element are F_x and F_y . The equations obtained are: [8b]

$$\begin{aligned}\rho b dx dy \frac{du_1}{dt} &= F_x \\ \rho b dx dy \frac{du_2}{dt} &= F_y\end{aligned}\tag{A.3}$$

The velocity change of the fluid element is brought about by the movement of position and the progress of time. It is expressed as: [8b]

$$du_1 = \frac{\partial u_1}{\partial t} dt + \frac{\partial u_1}{\partial x} dx + \frac{\partial u_1}{\partial y} dy\tag{A.4}$$

and

$$\frac{du_1}{dt} = \frac{\partial u_1}{\partial t} + u_1 \frac{\partial u_1}{\partial x} + u_2 \frac{\partial u_1}{\partial y}\tag{A.5}$$

In the y-direction the equation is equivalent. Equation A.5 and the equivalent equation in the y-direction are substituted into equation A.3 to give: [8b]

$$\begin{aligned}\rho \left(\frac{\partial u_1}{\partial t} + u_1 \frac{\partial u_1}{\partial x} + u_2 \frac{\partial u_1}{\partial y} \right) b dx dy &= F_x \\ \rho \left(\frac{\partial u_2}{\partial t} + u_1 \frac{\partial u_2}{\partial x} + u_2 \frac{\partial u_2}{\partial y} \right) b dx dy &= F_y\end{aligned}\tag{A.6}$$

The forces F_x and F_y include the body force, the pressure force and the viscous force. [8b]

$$F_{x,y} = B_{x,y} + P_{x,y} + S_{x,y}\tag{A.7}$$

Body forces are forces that act directly throughout the mass, such as the gravitational force. Putting X and Y as the components of such forces in the x and y directions, acting on the mass of the fluid gives:

$$\begin{aligned}B_x &= X \rho b dx dy \\ B_y &= Y \rho b dx dy\end{aligned}\tag{A.8}$$

For the gravitational force $X=0$ and $Y=-g$. [8b]

Both the pressure force and the viscous force are related to the velocity field, they generate stresses across any arbitrary surface within the fluid. [7]
Pressure force:

$$\begin{aligned}
P_x &= -\frac{\partial p}{\partial x} bdx dy \\
P_y &= -\frac{\partial p}{\partial y} bdx dy
\end{aligned}
\tag{A.9}$$

The viscous force is due to angular deformation of the fluid element. Viscous stresses oppose relative movements between fluid particles and so they oppose the deformation of fluid particles. The rate of deformation is described by the strain of the fluid. The stress depends on the strain and on the properties of the fluid. [7]

Viscous force:

$$\begin{aligned}
S_x &= \mu \left(\frac{\partial^2 u_1}{\partial x^2} + \frac{\partial^2 u_1}{\partial y^2} \right) bdx dy \\
S_y &= \mu \left(\frac{\partial^2 u_2}{\partial x^2} + \frac{\partial^2 u_2}{\partial y^2} \right) bdx dy
\end{aligned}
\tag{A.10}$$

The above expressions for the inertial force, the body force, the pressure force and the viscous force are substituted into equation A.6 to give the Navier-Stokes equations in two dimensions [8b]:

$$\begin{aligned}
\rho \left(\frac{\partial u_1}{\partial t} + u_1 \frac{\partial u_1}{\partial x} + u_2 \frac{\partial u_1}{\partial y} \right) &= \rho X - \frac{\partial p}{\partial x} + \mu \left(\frac{\partial^2 u_1}{\partial x^2} + \frac{\partial^2 u_1}{\partial y^2} \right) \\
\rho \left(\frac{\partial u_2}{\partial t} + u_1 \frac{\partial u_2}{\partial x} + u_2 \frac{\partial u_2}{\partial y} \right) &= \underbrace{\rho Y}_{\text{Body force}} - \underbrace{\frac{\partial p}{\partial y}}_{\text{Pressure}} + \underbrace{\mu \left(\frac{\partial^2 u_2}{\partial x^2} + \frac{\partial^2 u_2}{\partial y^2} \right)}_{\text{Viscous term}}
\end{aligned}
\tag{A.11}$$

$$\frac{\partial \rho}{\partial t} + \frac{\partial(\rho u_1)}{\partial x} + \frac{\partial(\rho u_2)}{\partial y} = 0
\tag{A.12}$$

Appendix B: Results of all simulations

Table 10: Simulation results for Model 1. The cooling rate and the surface temperature are averages of 80 % relative humidity and 100 % relative humidity.

Air velocity (m/s)	Air temp. (°C)	Fluid temp. (°C)	Average convective cooling (W)	Average surface temp. (K)	Heat transfer coefficient (W/m ² K)
1	10	25	34.4	297.89	4.67
		50	91.9	322.51	4.67
		75	149.3	347.07	4.67
	15	25	22.7	297.97	4.65
		50	79.8	322.59	4.64
		75	136.7	347.14	4.63
	20	25	11.2	298.04	4.63
		50	67.8	322.65	4.60
		75	124.3	347.21	4.60
2	10	25	45.7	297.85	6.22
		50	121.8	322.45	6.20
		75	197.8	246.97	6.20
	15	25	30.2	297.95	6.17
		50	105.9	322.52	6.16
		75	181.4	347.06	6.16
	20	25	15.0	298.02	6.17
		50	90.0	322.60	6.11
		75	165.0	347.13	6.11
3	10	25	53.5	297.85	7.29
		50	142.8	322.41	7.28
		75	231.9	346.91	7.28
	15	25	35.5	297.94	7.27
		50	124.1	322.50	7.23
		75	212.6	346.99	7.23
	20	25	17.6	298.02	7.25
		50	105.7	322.57	7.19
		75	193.6	347.08	7.18

Table 11: Simulation results for Model 2, cooling rates per 2 m², 100 % relative humidity.

Air velocity (m/s)	Air temp. (°C)	Fluid inlet temp. (°C)	Average surface temp. (°C)	Convective cooling (W)	Radiative cooling (W)	h _{rad} (W/m ² K)
1	10	25	23.60	127.0	135.4	4.98
		50	46.07	336.9	404.0	5.60
		75	68.27	544.2	731.4	6.28
	15	25	24.05	84.2	92.7	5.12
		50	46.53	292.6	362.5	5.75
		75	68.73	497.5	691.2	6.43
	20	25	24.53	41.9	47.6	5.26
		50	47.00	248.4	318.6	5.90
		75	69.19	452.5	648.6	6.59
2	10	25	23.39	166.6	133.3	4.98
		50	45.55	440.8	397.1	5.59
		75	67.43	712.1	718.0	6.25
	15	25	23.93	110.1	91.3	5.12
		50	46.07	382.8	356.4	5.74
		75	67.95	652.3	678.8	6.41
	20	25	24.46	55.0	46.9	5.26
		50	46.60	325.1	313.4	5.89
		75	68.49	592.5	673.3	6.94
3	10	25	23.26	193.3	131.8	4.97
		50	45.19	512.3	392.3	5.57
		75	66.85	827.7	708.8	6.23
	15	25	23.82	128.3	90.3	5.12
		50	45.75	444.7	352.3	5.73
		75	67.42	758.0	670.3	6.39
	20	25	24.41	63.9	46.4	5.26
		50	46.34	378.7	309.7	5.88
		75	68.00	689.3	629.5	6.56

Table 12: Simulation results for Model 2, cooling rates per 2 m², 80 % relative humidity.

Air velocity (m/s)	Air temp. (°C)	Fluid inlet temp. (°C)	Average surface temp. (°C)	Convective cooling (W)	Radiative cooling (W)	h_{rad} (W/m ² K)
1	10	25	22.90	120.5	272.0	4.55
		50	45.40	330.6	539.0	5.14
		75	67.59	537.9	864.6	5.80
	15	25	23.44	78.5	213.3	4.75
		50	45.93	287.0	481.6	5.36
		75	68.13	492.0	808.8	6.02
	20	25	23.92	36.3	166.2	4.91
		50	46.40	242.9	435.8	5.53
		75	68.61	447.2	764.2	6.20
2	10	25	22.70	158.0	269.9	4.54
		50	44.87	432.4	532.3	5.13
		75	66.77	703.9	851.4	5.77
	15	25	23.31	102.6	211.9	4.75
		50	45.48	375.5	475.7	5.35
		75	67.36	645.1	796.6	6.00
	20	25	23.86	47.6	165.6	4.91
		50	46.02	318.0	430.7	5.52
		75	67.91	585.5	753.1	6.18
3	10	25	22.58	183.4	268.5	4.54
		50	44.51	502.5	527.6	5.12
		75	66.19	818.1	842.4	5.76
	15	25	23.23	119.6	211.0	4.75
		50	45.17	436.2	471.6	5.34
		75	66.84	749.6	788.2	5.99
	20	25	23.82	55.4	165.1	4.91
		50	45.75	370.3	427.2	5.51
		75	67.43	681.1	745.4	6.17

Table 13: Results of the heat transfer efficiency assessment for the convection.

Air velocity (m/s)	Air temperature (°C)	Actual heat transfer (W)	Maximum heat transfer (W)	Effectiveness, ϵ_{NTU}
1	10	92	92.2	1.00
	15	79.9	79.5	1.01
	20	67.9	68.1	1.00
2	10	122.0	217.2	0.56
	15	106.0	187.6	0.57
	20	90.1	160.8	0.56
3	10	142.9	311.1	0.46
	15	124.2	268.5	0.46
	20	105.8	230.1	0.46

Table 14: Results of the heat transfer efficiency assessment for the radiation.

Air temp. (°C)	Ambient temp. (°C)	Surface temp. (K)	Actual radiative cooling (W)	$h_{rad, max}$	Maximum radiative cooling (W)	Effectiveness, ϵ_{NTU}
10	-7	317.66	527.6	5.86	668.0	0.79
	10	318.33	392.3	6.36	508.8	0.77
15	1	318.32	471.6	6.08	595.8	0.79
	15	318.91	352.3	6.50	455.0	0.77
20	7	318.90	427.2	6.26	538.4	0.79
	20	319.48	309.7	6.65	399.0	0.78

Table 15: Simulation results for a flat plate, wind velocity 2 m/s.

Air temperature (°C)	Plate temperature (°C)	Convective cooling (W)	h (W/m ² K)
10	25	60.5	8.07
	50	161.4	8.07
	75	262.3	8.07
15	25	39.9	7.98
	50	139.8	7.98
	75	239.7	7.99
20	25	19.8	7.92
	50	118.7	7.92
	75	217.6	7.92